Site-Directed Analysis of the Functional Domains in the Factor Xa Inhibitor Tick Anticoagulant Peptide: Identification of Two Distinct Regions That Constitute the Enzyme Recognition Sites

Christopher T. Dunwiddie,* Michael P. Neeper, Elka M. Nutt, Lloyd Waxman, Donna E. Smith, Kathryn J. Hofmann, Patricia K. Lumma, Victor M. Garsky, and George P. Vlasuk‡

Departments of Cellular and Molecular Biology, Pharmacology, Biological Chemistry, and Medicinal Chemistry, Merck Research Laboratories, West Point, Pennsylvania 19486

Received July 16, 1992; Revised Manuscript Received September 23, 1992

ABSTRACT: Recombinant tick anticoagulant peptide (rTAP) is a highly selective inhibitor of blood coagulation factor Xa. rTAP has been characterized kinetically as a slow, tight-binding, competitive inhibitor of the enzyme. We used an approach consisting of both recombinant, site-directed mutagenesis and solid-phase chemical synthesis to generate 31 independent mutations in rTAP to identify those regions of the molecule which contribute to the specific, high-affinity binding interaction with factor Xa. Our results demonstrate that the four amino-terminal residues of rTAP constitute the primary recognition determinant necessary for the formation of the high-affinity enzyme–inhibitor complex. The Arg residue in position three is probably not interacting with the S_1-specificity pocket of factor Xa in a substrate-like manner since substitution at this position with a D-Arg amino acid produced only a modest decrease in affinity (5-fold). An additional domain in the rTAP molecule located between residues 40 and 54 was identified as a probable secondary binding determinant. Interestingly, this region in rTAP shares significant amino acid sequence homology with a sequence in prothrombin immediately amino-terminal to the factor Xa cleavage site that generates meizothrombin. These observations indicate that specific segments within two different regions of the rTAP molecule contribute to the potent binding interaction between rTAP and factor Xa.

Inhibitors of serine proteases play an essential role in regulating the proteolytic activity associated with a variety of physiologic processes and pathological disorders including inflammation, emphysema, thrombosis, and thrombolysis (Neurath & Walsh, 1976; Perlmutter & Pierce, 1989). Although a diverse array of protein inhibitors of serine proteases has evolved in nature, most members have been grouped into families on the basis of sequence homologies, topological relationships, and the mechanism by which they bind with their target enzymes (Read & James, 1986; Laskowski & Kato, 1980). The largest group of protein inhibitors of serine proteases, characterized by the small Kunitz family of inhibitors, reacts with their cognate enzymes according to a standard mechanism in which a conformationally constrained, substrate-like binding loop is presented to the target enzyme (Laskowski & Kato, 1980). This canonical interaction is characterized by the formation of a stable enzyme–inhibitor complex which can undergo partial proteolytic hydrolysis at the reactive site peptide bond of the inhibitor (P_1–P_1'). This fully reversible hydrolysis reaction yields a modified form of the protein that remains a thermodynamically strong inhibitor which often exhibits a binding affinity similar to that of the native molecule. (Ardelt & Laskowski, 1991). Serpins comprise a second group of serine protease inhibitors consisting of a family of homologous, plasma-derived glycoproteins. Serpins inhibit their target enzymes by a mechanism similar to that described above with one major exception: the proteolytically modified forms of the serpins undergo a conformational rearrangement in which the two residues forming the reactive site bond of the intact inhibitor are shifted to opposite ends of the molecule. The modified protein is thermodynamically more stable but inactive as an inhibitor (Bode & Huber, 1992). The protease–serpin interaction is therefore not fully reversible as it is for the canonical inhibitors. Hirudin represents the sole member of a third type of inhibitor family that binds its target protease, thrombin, by a mechanism that is unique among serine protease inhibitors. Hirudin binds to thrombin at two separate sites: one site located adjacent to the active site and the other located along the fibrinogen binding "exosite" (Stone & Hofsteenge, 1986; Rydel et al., 1990). Hirudin does not occupy the specificity pocket of thrombin in a substrate-like manner, nor is it hydrolyzed during the inhibition process.

The complex series of catalytic reactions that comprise the coagulation cascade represents a proteolytic process that is highly regulated by endogenous serine protease inhibitors. A variety of exogenous protease inhibitors that disrupt coagulation hemostasis for the benefit of the host organism has also evolved in nature. One such protein, tick anticoagulant peptide (TAP),[1] is a potent and highly selective inhibitor of the serine protease coagulation factor Xa (fXa) (Waxman et al., 1990). A recombinant version of TAP (rTAP) has been characterized kinetically as a reversible, slow, tight-binding, competitive inhibitor of fXa (Neeper et al., 1990; Jordan et al., 1990). Although rTAP exhibits limited structural homology with the Kunitz family of serine proteases (Sardana et al., 1991), the putative reactive site cannot be assigned by analogy to other Kunitz inhibitors. This suggests that rTAP may interact with fXa by a mechanism more closely resembling that between hirudin and thrombin. In the present study, we utilized a directed mutagenesis approach to identify those amino acid

* To whom correspondence should be addressed.
‡ Current address: Corvas International, Inc., San Diego, CA 92121.

[1] Abbreviations: TAP, tick anticoagulant peptide; fXa, factor Xa; rTAP, recombinant tick anticoagulant peptide; RP-HPLC, reverse-phase high-pressure liquid chromatography; TBSA, Tris-buffered saline plus 0.1% bovine serum albumin; Boc, butyloxycarbonyl; PAM, phenylacetamidomethyl; PCR, polymerase chain reaction.

0006-2960/92/0431-12126$03.00/0

residues in rTAP which contribute to its high-affinity binding interaction with fXa. The possible mechanistic implications of these results and their relationship to the inhibitory mechanisms of other serine protease inhibitors are discussed.

EXPERIMENTAL PROCEDURES

Construction of Site-Directed rTAP Mutants. To facilitate preparation of single-stranded template DNA for most of the mutagenesis reactions, the TAP open reading frame was isolated from the yeast expression vector pKH4-TAP (Neeper et al., 1990) and inserted into the vector pKH4-3B (Carty et al., 1990) to generate the plasmid p3B-TAP. Briefly, the pKH4-3B vector was digested with *Sph*I, and the 3′-extensions were made flush-ended with T_4 DNA polymerase. Following digestion with *Bgl*II, the blunt *Bgl*II pKH4-3B vector was agarose gel purified. The TAP gene was amplified by polymerase chain reaction (PCR) with DNA oligomers that incorporated a *Bam*HI site downstream of the TAP gene on the 3′-end and a 5′-blunt end beginning with the DNA sequence encoding the first amino acid of TAP. The TAP gene was agarose gel purified and ligated with the pKH4-3B vector to yield p3B-TAP. The sequence of the final construct was confirmed by dideoxy sequence analysis (Sanger et al., 1977) using Sequenase (U.S. Biochemical Corp.). Most of the mutagenesis reactions were performed by the Kunkel method as modified by Hofmann et al. The *Escherichia coli* strain CJ236 [*dut*, *ung*, *thi*, *relA*; pCJ105(Cm^R)] was transformed with the p3B-TAP plasmid, and polyuracil-containing single-stranded p3B-TAP DNA was isolated following superinfection with the helper phage M13KO7 (Pharmacia). The single-stranded DNA served as the template for annealing of mutagenic primers specific for each mutation which were extended by DNA polymerase to produce double-stranded DNA. Following ligation, the double-stranded mutant DNAs were used to transform the *E. coli* strains MV1190 or DH5 which select for the mutant sequences due to the selective degradation of the uracil-containing parental strands. Mutations within the extreme amino or carboxy terminus of the TAP coding sequence were produced by polymerase chain reaction mutagenesis in which the desired mutation was included within the primer sequences used to amplify the DNA. The PCR product was digested with *Bam*HI, gel purified, and ligated with the *Bam*HI digested, dephosphorylated vector used to make pKH4-TAP. The DNA sequences of all the mutant clones were confirmed by direct sequence analysis.

Expression and Purification of Secreted rTAP Mutant Proteins. The *Saccharomyces cerevisiae* strain DMY6 (Mata/α, *ade1*, *ura3–52*, *his3::GAL10p–GAL4–ura3*, *leu2–2*, 112/leu2–04, cir^0/cir^0) was transformed with the mutant rTAP vectors according to the procedure of Hinnen et al. Transformants were selected on minimal medium agar plates without leucine, and clonal isolates were grown overnight in leucine minus minimal medium at 30 °C with adequate aeration. Cultures were diluted to a final volume of 250–500 mL, grown to an OD_{600} = 1.0–1.5, and then pelleted by low-speed centrifugation. TAP expression was induced by re-suspending the cell pellets in an equal volume of the leucine minus media containing 4% galactose. The induced cultures were propagated for an additional 48–72 h, and the resulting broth containing secreted rTAP was separated from the cells by centrifugation. The mutant rTAP proteins were purified essentially as described previously for wild-type rTAP with minor modifications (Neeper et al., 1990). Briefly, the harvested medium was diluted 5-fold with 50 mM sodium acetate, pH 4.0, and loaded at a flow rate of 50 mL/h onto a 10-mL column of S-Sepharose fast flow resin (Pharmacia) that had been preequilibrated with the same buffer. The column was washed with 10 column volumes of loading buffer and then eluted with a 100-mL linear gradient from 0 to 1 M NaCl in 50 mM sodium acetate, pH 4.0, and 1.5–2.0-mL fractions were collected. The fractions were assayed in parallel for fXa inhibitory activity and by Western blot analysis using a rabbit anti-TAP antibody. The peak fractions containing rTAP were pooled and lyophilized to dryness. The final purification of the rTAP mutant proteins was completed using preparative C_{18} reverse-phase HPLC as described (Neeper et al., 1990). The purified rTAP preparations were resuspended in HPLC-grade water and stored at 4 °C.

Analytical Evaluation of Purified Mutant rTAP Samples. rTAP protein concentrations and compositions were determined by replicate quantitative amino acid analysis of 20-h acid-hydrolyzed samples using a Beckman Model 6300 analyzer. Direct amino-terminal sequence analysis was resolved on an Applied Biosystems Model 470A sequenator. Electrophoretic analysis of rTAP samples was performed using the method of Schagger and Von Jagow. Analytical RP-HPLC analysis was accomplished using a 0.46- × 15-cm Vydac C_{18} column and a Perkin-Elmer Series 4 liquid chromatograph. The samples were loaded in aqueous 10% acetonitrile, 0.1% CF_3COOH at a flow rate of 1 mL/min and eluted with a linear gradient from 10% to 50% aqueous acetonitrile, 0.1% CF_3COOH over 40 min, and the eluant was monitored at 220 nm.

Peptide Synthesis and Purification. The stepwise solid-phase synthesis of all TAP peptides was carried out on an Applied Biosystems 430A automated peptide synthesizer using Boc-isoleucine-PAM resin and Boc-protected amino acids as described previously (Garsky et al., 1992). Peptides were deprotected and cleaved from the resin by treatment with hydrofluoric acid and refolded by air oxidation (Garsky et al., 1989). The crude product was purified by preparative HPLC using C_4 and C_{18} reverse-phase supports. The purity of the final products was confirmed to be greater than 98% by analytical RP-HPLC, amino acid composition analysis, amino-terminal sequence analysis, and mass spectroscopy.

Enzyme Assays and Measurement of the Kinetic Constants. Human fXa was prepared from human fX (Enzyme Research Laboratories, Inc.) as described previously (Dunwiddie et al., 1992; Bock et al., 1989), and the functional enzyme concentration was quantitated by active site titration using fluorescein mono-*p*-guanidinobenzoate. The enzymatic activity of human fXa was determined at 22 °C using the chromogenic substrate Spectrozyme FXa (methoxycarbonyl-D-cyclohexylglycyl-arginine-*p*-nitroanilide; American Diagnostics, Inc.) prepared as a stock solution in water. Reactions were measured in a 96-well microtiter plate (Dynatech) using a V-max kinetic microplate reader (Molecular Devices) by monitoring the increase in absorbance at 405 nm. All reactions were performed in a final volume of 220 μL of buffer consisting of 50 mM Tris-HCl, pH 7.5, 150 mM NaCl, 0.1% bovine serum albumin (TBSA) with a final concentration of 500 pM fXa and 300 μM substrate ($4K_m$). Inhibited, steady-state velocities were generated by preincubating fXa with increasing concentrations of rTAP (0.05–10 nM) for 40 min to allow equilibration of the enzyme–inhibitor (EI) complex. The reaction was initiated by the addition of substrate, and the residual enzyme activity was determined by measuring the initial velocity of the reaction over a 5-min period. The equilibrium dissociation constants were calculated by fitting the steady-state velocities to Morrison's equation for tight-

binding inhibition using nonlinear regression analysis (Morrison, 1969; Jordan et al., 1990):

$$V_s/V_0=\{(E_t - I_t - K_i) + [(I_t + K_i - E_t)^2 + 4K_iE_t]^{1/2}\}/2E_t$$

where K_i is the dissociation constant for the EI complex, V_s is the inhibited steady-state velocity, V_0 is the control velocity (no inhibitor), I_t is the total inhibitor concentration, and E_t is the total fXa concentration. Reiterative fits of the steady-state velocity data yielded independent measurements of K_i values with less than 15% error. Dissociation constants were determined in triplicate and expressed as the average ± SEM. The kinetic parameters for two of the rTAP mutants, D47N and D54N, could not be accurately determined by measuring the steady-state velocities from preequilibrated EI complexes. The dissociation rates of the EI complex for these two mutant proteins were sufficiently rapid that dissociation of the EI complex over the time course of the assay became significant. Therefore, the kinetic constants for these mutant rTAP proteins were determined by generating slow-binding progress curves in which reactions were initiated by the addition of enzyme to mixtures of substrate and inhibitor. The progress curves generated were fit directly by nonlinear regression to the integrated first-order rate equation described by Williams and Morrison (1979) and Cha (1975):

$$P = V_s t + (V_0 - V_s)(1 - e^{-k_{obs}t})/k_{obs}$$

where V_0 is the initial reaction velocity, V_s is the final steady-state velocity, and k_{obs} is the apparent first-order rate constant which describes the equilibration from the initial to the final steady state. It has been shown previously that over the range of inhibitor concentrations analyzed in these studies (0.1–20 nM) rTAP inhibits fXa according to a one-step, slow-binding mechanism described by the scheme outlined below (Jordan et al., 1990).

$$\begin{array}{ccccc} E + S & \rightleftharpoons & ES & \longrightarrow & P \\ + & & & & \\ I & & & & \\ k_1 \downarrow\uparrow k_{-1} & & & & \\ EI & & & & \end{array}$$

This scheme can be described by the equation which relates the k_{obs} values determined above to the rate constants describing formation and dissociation of the EI complex (Morrison, 1982):

$$k_{obs} = k_1[I]/(1 + [S]/K_m) + k_{-1}$$

where k_1 is the second-order rate constant describing formation of EI and k_{-1} is the dissociation rate constant, and the equilibrium dissociation constant can be calculated from the expression $K_i = k_{-1}/k_1$. The k_{obs} values determined by fitting the progress curves obtained over a wide range of inhibitor concentrations were fit to the equation above by nonlinear regression. The kinetic constants k_{-1}, k_1, and K_i were determined for three independent sets of data for wild-type rTAP and each mutant rTAP protein and expressed as the average ± SEM. Two rTAP mutants, R3K and R3N, failed to display slow-binding kinetics and exhibited inhibitory activity only over a much higher concentration range such that they were no longer classified as tight-binding inhibitors. Accordingly, the dissociation constants for these mutants were determined by analyzing steady-state velocity data using inverse plots and Dixon plots (Dixon, 1953). The values reported represent the average ± SEM of three independent determinations.

Table I: Effects of Site-Directed Mutagenesis of All Charged Residues within rTAP on the Inhibition Constant (K_i) with Human Factor Xa

rTAP mutant	K_i[a] (nM)	x-fold change[b]
wild type	0.1353 ± 0.0045	1.0
R3N	5680 ± 200	+41 981
R3K	156 ± 5.2	+1 153
R9N	0.2110 ± 0.0012	+1.6
R23N	0.1480 ± 0.0101	+1.1
R27N	0.1600 ± 0.0061	+1.2
R53N	0.0925 ± 0.0070	−1.5
K7N	0.1756 ± 0.0052	+1.3
K30N	0.2164 ± 0.0058	+1.6
D10N	0.1030 ± 0.0018	−1.3
D13N	0.1928 ± 0.0071	+1.4
D16N	0.1301 ± 0.0015	1.0
D16R	0.1700 ± 0.0076	+1.3
D16K	0.1168 ± 0.0038	−1.2
D34N	0.0942 ± 0.0016	−1.4
D42N	0.2769 ± 0.0072	+2.1
E14Q	0.1350 ± 0.0048	1.0
E19Q	0.1806 ± 0.0015	+1.3
E22Q	0.1233 ± 0.0042	−1.1
E41Q	0.1872 ± 0.0041	+1.4

[a] Reaction conditions and methods for calculating K_i are described in Experimental Procedures under Enzyme Assays and Measurement of the Kinetic Constants. Values are expressed as the average ± SEM, n = 3. [b] x-fold change is expressed relative to that of wild-type rTAP.

RESULTS

Kinetic Analysis of Site-Directed rTAP Mutants. Each rTAP mutant was purified from yeast-conditioned media by a combination of S-Sepharose and RP-HPLC chromatography. The amino acid substitutions in each rTAP mutant were verified at the protein sequence level by direct amino-terminal sequence analysis of either the purified proteins or staphylococcal V8 and endoprotease Lys-C generated peptide fragments containing the mutated residues (data not shown). Each mutant protein preparation was shown to be at least 95% pure by a combination of amino acid composition analysis, analytical RP-HPLC analysis, and amino-terminal sequence analysis as described previously (Neeper et al., 1990).

Structural comparisons between rTAP and other serine protease inhibitors reveal limited structural homology to the Kunitz family of inhibitors (Waxman et al., 1990). The topological relationships between the three disulfide bonds in rTAP are the same as those in the prototypical Kunitz inhibitor, bovine pancreatic trypsin inhibitor; however, invariant spacing between the cysteine residues in the two inhibitors must be accommodated (Sardana et al., 1991). All members of the Kunitz inhibitor family exhibit a positively charged P_1 reactive site residue immediately adjacent to the second cysteine residue in the primary sequence. In contrast, rTAP has a negatively charged aspartic acid residue in the comparable position. This observation suggests a possible explanation for its inability to inhibit a variety of trypsin-like serine proteases (Waxman et al., 1990). To investigate the possibility that rTAP may be conformationally similar to the Kunitz inhibitor family with a unique specificity for fXa, the aspartic acid residue at position 16 in rTAP was independently mutated to a positively charged arginine or lysine. The mutants D16R and D16K were assayed for their abilities to inhibit both fXa and trypsin. As shown in Table I, neither mutation resulted in a loss in binding affinity for fXa. In addition, neither mutant acquired the ability to inhibit trypsin even at a 300:1 molar excess of inhibitor over

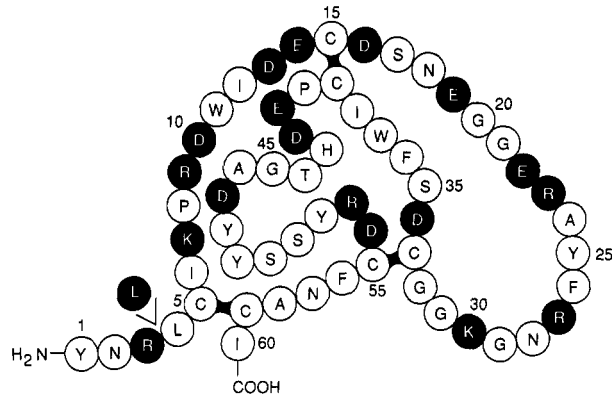

FIGURE 1: Summary of rTAP structure and site-directed mutants. The primary structure of rTAP is shown with the assignment of the three disulfide bridges indicated. Amino acids are identified by the single-letter code, and all those residues which were independently mutated are in black. The single leucine insertion mutation between residues three and four is indicated.

enzyme (data not shown). Attempts to show hydrolysis of D16R or D16K by either trypsin or fXa were unsuccessful, demonstrating that these mutants were not acting as limited proteolytic substrates for the enzymes (G. Vlasuk, unpublished results). These results suggest that rTAP may have a distinct three-dimensional conformation compared to members of the Kunitz family of inhibitors despite sharing a similar disulfide arrangement and may explain why rTAP does not inhibit fXa according to the mechanism typical of the Kunitz family of inhibitors.

Since fXa exhibits a strict specificity for an arginine in the P_1 position of its substrates, the next series of mutants focused on the five arginine residues in rTAP. It was postulated that one of these arginines may serve as the P_1 residue of the inhibitor's reactive site (Figure 1). As shown in Table I, the independent substitution of each arginine residue at positions 9, 23, 27, or 53 with an uncharged asparagine did not cause a significant increase in the dissociation constant. Mutant R53N, however, exhibited a modest but reproducible increase in fXa inhibitory potency (see below). In contrast, mutation of the arginine residue to an asparagine residue at position 3 resulted in a greater than 40 000-fold decrease in the fXa binding affinity of this mutant as reflected by a dissociation constant of 5.68 μM (Table I). To investigate the importance of maintaining a positively charged residue at this position, Arg-3 was mutated to a lysine. This mutation resulted in a dissociation constant of 156 nM (Table I), a loss in affinity of approximately 1000-fold, which confirms the requirement for a positively charged residue at this position with a guanidinium side chain being preferred over an ϵ-amino side chain. Mutation of the other two positively charged residues in rTAP, Lys-7 and Lys-30, to uncharged asparagine residues produced no significant loss in binding affinity with fXa. These results suggest that the peptide bond between Arg-3 and Leu-4 may represent the reactive site bond in rTAP; however, attempts to demonstrate hydrolysis of rTAP by fXa at this site have been unsuccessful (G. Vlasuk, unpublished results). Alternatively, Arg-3 may form a critical salt linkage with one of the 11 negatively charged residues in rTAP and thus provide a primary structural constraint necessary for maintaining the proper conformation of the molecule. To investigate this possibility, all glutamate and aspartate residues were independently mutated to uncharged glutamine and asparagine residues, respectively (Figure 1). Analysis of the binding affinity between each mutant and fXa revealed that only three mutations, D42N, D47N, and D54N, caused a greater than

Table II: Slow Binding Kinetic Constants Measured for Wild-Type rTAP and the Mutants D47N and D54N with Human Factor Xa

rTAP mutant	equilibrium binding and rate constants[a]		
	k_{on} [$(M \cdot s)^{-1} \times 10^{-6}$]	k_{off} ($s^{-1} \times 10^4$)	K_i (nM)
wild type	3.41 ± 0.11	5.24 ± 0.38	0.154 ± 0.007 (1.0)
D47N	2.25 ± 0.06	10.71 ± 1.81	0.476 ± 0.081 (3.1)
D54N	2.30 ± 0.07	13.52 ± 2.31	0.588 ± 0.092 (3.8)

[a] Reaction conditions and methods for measuring and calculating the slow-binding kinetic constants are described in Experimental Procedures under Enzyme Assays and Measurement of the Kinetic Constants. Values are expressed as the average ± SEM, $n = 3$. Values in parentheses represent the x-fold increase in the equilibrium dissociation constant relative to the value determined for wild-type rTAP.

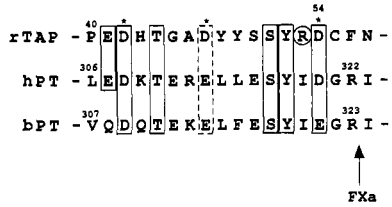

FIGURE 2: Alignment of homologous amino acid residues between rTAP and prothrombin. The region of rTAP between residues 40 and 57 is aligned with the homologous region in human (hPT) and bovine (bPT) prothrombin. Identical residues are enclosed in solid boxes and conserved residues are enclosed in dashed boxes. The fXa cleavage site in prothrombin leading to the generation of meizothrombin is shown. Those aspartic acid residues which yield reduced binding affinity with fXa when mutated are indicated by asterisks, and the nonconserved arginine residue at position 53 is circled.

2-fold loss in binding affinity relative to that of wild-type rTAP (Tables I and II). The loss in affinity for the two mutants D47N and D54N was primarily accounted for by an increase in the value of their dissociation rate constants (Table II). These results demonstrate that none of the individual aspartate and glutamate mutations resulted in a decreased binding affinity of comparable magnitude as that of the R3N mutation. Therefore, the arginine residue at position 3 is probably directly involved in the high-affinity binding interaction with fXa and does not simply maintain the proper structure of rTAP via a salt linkage. Interestingly, the three mutated residues D42N, D47N, and D54N are located within a 15 amino acid stretch or rTAP that shares significant amino acid sequence homology with a segment in prothrombin immediately amino-terminal to the fXa cleavage site responsible for the generation of meizothrombin (Figure 2). These three acidic residues are highly conserved between rTAP and both human and bovine prothrombin (Figure 2, asterisks). Two additional mutated residues within this region of rTAP, Glu-41 and Arg-53, are also worthy of note. Position 41 in rTAP, and the homologous position in human prothrombin, is occupied by a glutamate residue whereas bovine prothrombin contains an uncharged glutamine at this position. This suggests that conservation of a negatively charged residue at this site is not critical. Consistent with this implication, the E41Q rTAP mutant revealed no significant loss in affinity for fXa (Table I). Position 53 in rTAP contains a positively charged arginine residue whereas both human and bovine prothrombin contain an uncharged isoleucine residue in the corresponding location (Figure 2). Mutation of this position in rTAP to an uncharged asparagine residue resulted in a modest but consistent decrease in the equilibrium constant which suggests that the charged residue at this position in rTAP may not be optimal (Table I).

Table III: Relative Human Factor Xa Inhibitory Potency of Amino-Terminally Truncated and D-Arg-3-Substituted Synthetic TAP Mutants

TAP mutant	IC_{50} value[a]	x-fold increase[b]
TAP 1–60	0.36 nM	1
TAP 2–60	4.45 μM	12 361
TAP 3–60	>300 μM	>833 333
TAP 4–60	22 μM	61 111
TAP 5–60	>300 μM	>833 333
[D-Arg-3]TAP 1–60	1.95 nM	5
[D-Arg-3]TAP 2–60	9.81 μM	27 250
[D-Arg-3]TAP 3–60	>200 μM	>555 555
[D-Arg-3]TAP 4–60	60 μM	166 666
[D-Arg-3]TAP 5–60	>300 μM	>833 333

[a] Inhibited steady-state velocities were determined following preequilibration of 0.5 nM human factor Xa with increasing concentrations of each peptide. Residual enzyme activity was determined following the addition of 300 μM substrate as described in Experimental Procedures. The upper concentration limit of each peptide was limited both by peptide solubility and by the quantity of peptide. The values represent the average of two independent determinations. [b] Values are expressed as x-fold increase relative to 1–60 synthetic TAP.

Synthetic TAP Mutants. A series of amino-terminally truncated TAP mutants were synthesized by solid-phase techniques to further investigate the role played by the amino-terminal portion of TAP in its binding with fXa. Deletion of the amino-terminal tyrosine in TAP (Figure 1) resulted in a greater than 12 000-fold loss in fXa inhibitory activity relative to that of synthetic full-length TAP (Table III). The further sequential truncation of residues 2–4 caused a concomitant decrease in inhibitory potency. It is interesting to note that TAP(4–60) exhibits a 10-fold increase in inhibitory potency relative to that of TAP(3–60). This result suggests that although a positive charge at position 3 is important for the function of the full-length inhibitor, its presence as the amino-terminal residue is detrimental. We also investigated the effects of substituting the Arg-3 residue with a D-Arg amino acid. As shown in Table III, the D-Arg-3 TAP mutant exhibited a modest 5-fold loss in fXa inhibitory potency relative to that of wild-type TAP. Thus, the overall positioning of the guanidinium group at position 3 is not as critical to inhibitor function as the presence of this charged moiety. The sequential truncation of the D-Arg-3-containing TAP mutants revealed the same pattern of loss of inhibitory function as that of the L-Arg-3-containing series (Table III). These results further demonstrate that the amino-terminal portion of TAP, spanning residues 1–4, plays a critical role in the formation of the high-affinity fXa–TAP inhibitory complex.

Insertion Mutation between Amino Terminus and the Prothrombin-Like Sequence of rTAP. The previous results demonstrate that binding interactions occur between fXa and two different regions of the TAP molecule. The spatial constraints placed upon these two distinct binding regions were examined through the creation of a site-directed mutant in which a single leucine residue was inserted between rTAP residues Arg-3 and Leu-4 (Figure 1). Activity analysis of this mutant revealed a greater than 150 000-fold loss in inhibitory potency (IC_{50} = 50 μM) relative to that of wild-type rTAP (IC_{50} = 0.33 nM). This indicates that the amino-terminal binding site and the prothrombin-like binding site in rTAP must remain in a highly constrained and specific spatial conformation in order to support high-affinity binding with fXa.

DISCUSSION

The results of this study indicate that two distinct regions in the TAP molecule contribute to the high-affinity binding interaction with fXa. Recent results from a study in which the rapid kinetics of fXa inhibition were examined revealed that the inhibition of fXa by rTAP is best characterized by a two-step kinetic mechanism (Jordan et al., 1992). An initial low-affinity enzyme–inhibitor complex rapidly forms then slowly rearranges or binds at additional contact points to yield the final high-affinity enzyme–inhibitor complex (Jordan et al., 1992). These authors also showed that rTAP can form a low-affinity complex with modified fXa noncovalently blocked at the active site with *p*-aminobenzamidine or covalently blocked with dansyl-L-glutamyl-glycyl-L-arginine chloromethyl ketone, which demonstrates that rTAP binds to sites on fXa distinct from the active site pocket of the enzyme. The most direct interpretation of our results within the context of the kinetic data is that two distinct regions in TAP interact with different binding sites on fXa according to a two-step process. This model predicts that the prothrombin-like sequence spanning residues 40–54 initially interacts with an extended S subsite on fXa in a substrate-like manner to yield a low-affinity complex. This initial complex positions the amino-terminal tail of TAP, minimally including residues Tyr-1 and Arg-3, into the proper orientation for a secondary high-affinity binding interaction with fXa. The results obtained with the D-Arg-3-substituted mutant suggest that this residue is not binding within the active site pocket of fXa in a substrate-like manner; however, we are unable to discern from our results whether the amino-terminal portion of TAP binds fXa near the active site or at a more distant site on the molecule. The similar values measured for the dissociation constant between wild-type rTAP and active site blocked fXa (5.9 μM; Jordan et al., 1992) and the dissociation constant between the R3N rTAP mutant and fXa (5.7 μM) provide suggestive evidence for the binding of the amino-terminal portion of rTAP at a site physically near the active site of fXa. The relatively good inhibitory potency retained by the D-Arg-3 mutant indicates that the five amino-terminal residues of TAP may be arranged in a β-turn and antiparallel sheet structure, a conformation that would allow the charged guanidinium group of Arg-3 to occupy a similar, although not identical, spatial arrangement in both a D- and L-amino acid configuration.

The postulated binding interaction between TAP and fXa most closely resembles the mechanism of inhibition exhibited by hirudin with its target protease, thrombin. We cannot conclude from our data however, whether TAP binds to a site on fXa analogous to the "exosite" occupied by hirudin on thrombin or simply binds at multiple contact points near the active site cleft of fXa. Despite the similarities in their inhibitory mechanisms, two observations would suggest that the binding interaction between TAP and fXa is fundamentally different from that between hirudin and thrombin. First, the secondary binding determinant in TAP, composed of the prothrombin-like sequence, is predicted to bind to an extended S subsite on fXa rather than an extended S′ subsite like the exosite on thrombin. And second, hirudin binds to the thrombin exosite in an ionic strength-dependent manner whereas the binding of TAP to fXa is not affected by changes in the ionic strength (Jordan et al., 1990, 1992). Therefore, if TAP binds to a site on fXa analogous to the exosite on thrombin, the predominant binding interaction must not be ionic.

ACKNOWLEDGMENT

We thank the following people for their respective contributions: John Rodkey for amino acid sequence analysis;

Kathy Short for oligonucleotide synthesis; David Kolodin and Mei Tang for amino acid composition analysis; and Dr. Ruth Nutt for many helpful discussions.

REFERENCES

Ardelt, W., & Laskowski, M., Jr. (1991) *J. Mol. Biol. 220*, 1041–1053.

Bock, P. E., Craig, P. A., Olson, S. T., & Singh, P. (1989) *Arch. Biochem. Biophys. 273*, 375–388.

Bode, W., & Huber, R. (1992) *Eur. J. Biochem. 204*, 433–451.

Carty, C. E., Hofmann, K. J., Keller, P. M., Polokoff, M. A., Lynch, R. J., Keech, B. J., Gould, R. J., Maigetter, R. Z., & Schultz, L. D. (1990) *Biotechnol. Lett. 12*, 879–884.

Cha, S. (1975) *Biochem. Pharmacol. 24*, 2177–2185.

Dixon, M. (1953) *Biochem. J. 55*, 170–178.

Dunwiddie, C. T., Vlasuk, G. P., & Nutt, E. M. (1992) *Arch. Biochem. Biophys. 294*, 647–653.

Garsky, V. M., Lumma, P. K., Freidinger, R. M., Pitzenberger, S. M., Randall, W. C., Veber, D. F., Gould, R. J., & Friedman, P. A. (1989) *Proc. Natl. Acad. Sci. U.S.A. 86*, 4022–4026.

Garsky, V. M., Lumma, P. K., Waxman, L., Vlasuk, G. P., Ryan, J. A., Veber, D. F., & Freidinger, R. M. (1992) in *Peptides: Chemistry and Biology* (Smith, J. A. & Rivier, J. E., Eds.) pp 908–910, ESCOM, Leiden.

Hinnen, A., Hicks, J. B., & Jink, G. R. (1978) *Proc. Natl. Acad. Sci. USA 75*, 1929–1933.

Hofmann, K. J., Nutt, E. M., & Dunwiddie, C. T. (1992) *Biochem. J.* (in press).

Jordan, S. P., Waxman, L., Smith, D. E., & Vlasuk, G. P. (1990) *Biochemistry 29*, 11095–11100.

Jordan, S. P., Mao, S. S., Lewis, S. D., & Shafer, J. A. (1992) *Biochemistry 31*, 5374–5380.

Laskowski, M., Jr., & Kato, I. (1980) *Annu. Rev. Biochem. 49*, 593–626.

Morrison, J. F. (1969) *Biochim. Biophys. Acta 185*, 269–286.

Morrison, J. F. (1982) *Trends Biochem. Sci. 7*, 102–105.

Neeper, M., Waxman, L., Smith, D., Schulman, C., Sardana, M., Ellis, R. W., Schaffer, L., Siegl, P. K. S., & Vlasuk, G. P. (1990) *J. Biol. Chem. 265*, 17746–17752.

Neurath, H., & Walsh, K. A. (1976) *Proc. Natl. Acad. Sci. U.S.A. 73*, 350–357.

Perlmutter, D. H., & Pierce, J. A. (1989) *Am. J. Physiol. 257*, L147–L162.

Read, R., & James, M. N. (1986) in *Proteinase Inhibitors* (Barret, A. J., & Salvesen, G., Eds.) Vol. 12, pp 301–336, Elsevier, New York/Amsterdam.

Rydel, T. J., Ravichandran, K. G., Tulinsky, A., Bode, W., Huber, R., Roitsch, C., & Fenton, J. W. (1990) *Science 249*, 277–280.

Sanger, F., Nicklen, S., & Coulson, A. R. (1977) *Proc. Natl. Acad. Sci. U.S.A. 74*, 5463–5465.

Sardana, M., Sardana, V., Rodkey, J., Wood, T., Ng, A., Vlasuk, G. P., & Waxman, L. (1991) *J. Biol. Chem. 266*, 13560–13563.

Schagger, H., & Von Jagow, G. (1987) *Anal. Biochem. 166*, 368–379.

Stone, S. R., & Hofsteenge, J. (1986) *Biochemistry 25*, 4622–4628.

Waxman, L., Smith, D. E., Arcuri, K. E., & Vlasuk, G. P. (1990) *Science 248*, 593–596.

Williams, J. W., & Morrison, J. F. (1979) *Methods Enzymol. 63*, 437–467.